



**HAL**  
open science

## Oxidative radicals (HO• or N3•) induce several di-tyrosine bridge isomers at the protein scale

Anouchka Gatin, Isabelle Billault, P Duchambon, Guillaume van Der Rest, Cécile Sicard-Roselli

### ► To cite this version:

Anouchka Gatin, Isabelle Billault, P Duchambon, Guillaume van Der Rest, Cécile Sicard-Roselli. Oxidative radicals (HO• or N3•) induce several di-tyrosine bridge isomers at the protein scale. *Free Radical Biology and Medicine*, 2020, 20, pp.S0891. 10.1016/j.freeradbiomed.2020.10.324 . hal-04056206

**HAL Id: hal-04056206**

**<https://hal.science/hal-04056206>**

Submitted on 22 Jul 2024

**HAL** is a multi-disciplinary open access archive for the deposit and dissemination of scientific research documents, whether they are published or not. The documents may come from teaching and research institutions in France or abroad, or from public or private research centers.

L'archive ouverte pluridisciplinaire **HAL**, est destinée au dépôt et à la diffusion de documents scientifiques de niveau recherche, publiés ou non, émanant des établissements d'enseignement et de recherche français ou étrangers, des laboratoires publics ou privés.



Distributed under a Creative Commons Attribution - NonCommercial 4.0 International License

## **Oxidative radicals (HO<sup>•</sup> or N<sub>3</sub><sup>•</sup>) induce several di-tyrosine bridge isomers at the protein scale**

Anouchka Gatin<sup>a</sup>, Isabelle Billault<sup>a</sup>, Patricia Duchambon<sup>b</sup>, Guillaume Van der Rest<sup>a</sup> and Cécile Sicard-Roselli<sup>a</sup>

<sup>a</sup> Université Paris-Saclay, CNRS, Institut de Chimie Physique UMR 8000, 91405 Orsay Cedex, France

<sup>b</sup> CNRS UMR9187, INSERM U1196, Institut Curie, Université Paris Saclay, 91405 Orsay Cedex, France

\*Corresponding author: Cécile Sicard-Roselli ([cecile.sicard@universite-paris-saclay.fr](mailto:cecile.sicard@universite-paris-saclay.fr))

### **Highlights**

- UPLC-MS optimized separation highlights new additional di-tyrosine bridges induced by hydroxyle or azide radicals
- **Oxidative radicals (HO<sup>•</sup> or N<sub>3</sub><sup>•</sup>) produced by gamma radiolysis** lead to five di-tyrosine bridges in a full-length protein ( $\Delta$ 25-centrin 2)
- At least four covalent dimers of the tyrosine amino acid are formed under the effect of oxidizing radicals

### **Abstract**

Among protein oxidative damages, di-tyrosine bridges formation has been evidenced in many neuropathological diseases. Combining oxidative radical production by gamma radiolysis with very performant chromatographic separation coupled to mass spectrometry detection, we brought into light new insights of tyrosine dimerization. Hydroxyl and azide radical tyrosine oxidation leading to di-tyrosine bridges formation was studied for different biological compounds: a full-length protein ( $\Delta$ 25-centrin 2), a five amino acid peptide (KTSLY) and free tyrosine. We highlighted that both radicals generate high proportion of dimers even for low doses. Surprisingly, no less than five different di-tyrosine isomers were evidenced for the protein and the peptide. For tyrosine alone, at least four distinct dimers were evidenced. These results raise some questions about their respective role *in vivo* and hence their relative toxicity. Also, as di-tyrosine is often used as a biomarker, a better knowledge of the type of dimer detected *in vivo* is now required.

### **Graphical abstract**

**Keywords:** *Di-tyrosine; Human centrin 2; Mass spectrometry; Oxidative stress; Hydroxyl radical*

**Funding:** This research did not receive any direct specific grant from funding agencies in the public, commercial or not-for-profit sectors. Access to the UPLC-MS was funded as the MOBICS project funded by a DIM Analytics program from the Ile-de-France region.

## 1. Introduction

In the context of oxidative stress inducing protein damages, tyrosine is known as one of the most sensitive residues [1, 2]. Whatever the conditions used to mimic a stress (UV light, gamma rays, metal catalysed oxidation...) on peptides or proteins containing tyrosine residues, di-tyrosine, formed by the elimination of two hydrogens, is one of the oxidation product[3-8]. Tyrosine dimerization has already been extensively studied, both from a fundamental [9-14] and a biological [8, 15-18] point of view. Di-tyrosine bridges are found in many structural protein hydrolysates and can therefore be used as a specific biomarker of aging [19, 20] or oxidative pathologies [21, 22]. In a broad number of neurodegenerative diseases, they were also identified [23] such as in  $\beta$ -Amyloid or  $\alpha$ -synuclein fibrils, responsible for Alzheimer and Parkinson diseases, respectively. In neurotoxic fibrils, di-tyrosine bridges were identified and proposed to be responsible for fibrils stabilization [24, 25]. Covalent cross-linking in proteins through di-tyrosine is regularly evidenced by the use of di-tyrosine targeted antibodies [8, 26] or by fluorometry, as di-tyrosine display specific fluorescence properties [18, 27, 28].

In all these biological contexts, only one type of tyrosine dimer in proteins is generally evoked. However, among approaches developed to decipher its formation mechanism, pulse radiolysis and photochemistry experiments [12, 29, 30] showed different radical reactions pathways raising the possibility to produce several isomers of tyrosine dimers in the presence of oxidizing radicals. At least two types of dimers are mentioned in the literature and were structurally characterized: *ortho-ortho* di-tyrosine named also *o,o'*-di-tyrosine, and *iso* di-tyrosine [12, 31-34] (Scheme 1). Thus, although chemical literature points out two possible forms, biological literature mostly only considers the *o,o'*-di-tyrosine when considering protein cross-linking.

In this work, coupling specific and quantitative radical production to Ultra Performance Liquid Chromatography (UPLC) analysis equipped with high resolution mass detection (Q-ToF (Quadrupole Time of Fly)), we studied tyrosine oxidative dimerization for both a protein and the isolated amino acid. Hydroxyl radicals ( $\text{HO}^\bullet$ ), produced during cellular oxidative stress, can oxidize both the backbone and side chain residues [35] of proteins according to its extremely high redox potential (2.78 V vs. SHE (Standard Hydrogen Electrode)). Azide radicals ( $\text{N}_3^\bullet$ ), whose redox potential is lower (1.3 V vs. SHE) are regularly used in protein oxidation studies because they can mimic part of the oxidative damages of  $\text{HO}^\bullet$ . They mainly oxidize tryptophan and tyrosine residues and in some specific conditions methionine [36, 37]. Therefore we compared di-tyrosine formation for both radicals,  $\text{HO}^\bullet$  and  $\text{N}_3^\bullet$ .

Human centrin 2 (Hscen2), a 20 kDa calcein protein implicated in various biological processes such as DNA (Deoxyribonucleic Acid) nucleotide excision repair [38] and centrosome duplication [39], appears as a good candidate for this study. Indeed, human centrin 2 contains a single tyrosine in the C-terminal position but neither cysteine nor tryptophan. Thus the redox reactivity of this protein should mainly concern its tyrosinyl residue. When exposed to oxidative conditions with azide radicals, the protein oligomerization [40, 41] between the C-terminal tyrosines of each monomer assembly is almost stoichiometric. We then wish to compare both with azide and hydroxyl radicals tyrosine and Hscen2 behaviours upon oxidation.

Considering the importance of di-tyrosine bridges *in vivo* when proteins are oxidatively damaged, we looked for possible existence of several di-tyrosine dimers in a full-length protein,  $\Delta 25$ -centrin 2. This truncated form of Hscen 2 dimerizes just as efficiently as the full-length protein. It is easier to handle *in-vitro* without risking to self assemble [42].

Based on specific and quantitative radical production, coupled to very performant chromatographic separation equipped with a very sensitive mass spectrometry (MS) detection, this study evidences the formation of several different di-tyrosine bridges in a protein submitted to oxidative radicals, which is a new knowledge on the reactivity of these species. The most noticeable results presented in this paper are i) the important proportion of protein dimers for both radicals, ii) the formation of at least 5 covalent di-tyrosine bridges for a protein and a 5 amino acids peptide, iii) the formation of at least 4 different covalent dimers for the isolated tyrosine.

## **2. Materials and Methods**

### *2.1. Sample preparation*

All samples were prepared with purified water (Elga Maxima system 18.2 M $\Omega$ .cm).

### *2.2. Tyrosine and peptide*

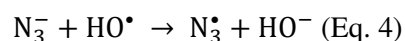
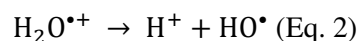
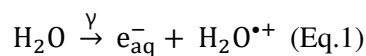
L-Tyrosine was purchased from Sigma-Aldrich, purity > 99%. L-KTSLY peptide was purchased from ProteoGenix, purity 98%.

### *2.3. Protein production and purification*

Experiments were performed on a fragment of Human centrin 2 containing the sequence 26-172 with an additional N-terminal methionine residue, named  $\Delta 25$ -centrin 2 (M=17062 g.mol<sup>-1</sup>). Its production and purification in *E.Coli* was already described in Blouquit et al. [40].

### *2.4. Gamma radiolysis experiments*

Gamma irradiation of water leads to water ionization and excitation then inducing mainly the formation of hydrated electron (Eq. 1) and hydroxyl radical (Eq. 2). Under N<sub>2</sub>O atmosphere, e<sub>aq</sub><sup>-</sup> is scavenged to form HO• (Eq. 3). In the presence of N<sub>3</sub><sup>-</sup>, HO• are scavenged to form N<sub>3</sub>• (Eq. 4):



For radiolysis experiments, 50 μM solutions were prepared in 10 mM phosphate buffer at pH 7.0. All samples were flushed with N<sub>2</sub>O gas for forty minutes, avoiding bubbling in the solution in order to obtain a complete saturation of the samples. To provide azide radicals, NaN<sub>3</sub>, 10 mM final concentration, was added. Gamma radiolysis was performed on a panoramic <sup>60</sup>Co source. The dose rate fixed at 10 Gy.min<sup>-1</sup> was determined using a Fricke dosimeter [43]. 1 Gray (Gy) represents 1 J.kg<sup>-1</sup>. Under gamma irradiation, formation yield of HO• or solvated electron is 0.28 μmol.J<sup>-1</sup>. Under our conditions i.e. N<sub>2</sub>O, solvated electron is transformed in HO• and then 1 Gy generates 0.56 μmol.L<sup>-1</sup> of HO• or N<sub>3</sub>•.

### 2.5. Electrophoresis gels

Sodium dodecyl sulfate polyacrylamide gel electrophoresis (SDS-PAGE) was run on 12% acrylamide gels (Criterion TGX, BioRad) with a Tris-Glycine buffer. 10 μg of protein were deposited in each well. Staining was performed with Coomassie Blue R-250. Gel analysis was performed with ImageJ software.

### 2.6. Tryptic cleavage

For trypsin treatment after irradiation, Δ25-centrin 2 was first dialysed against 10 mM ammonium acetate buffer, using the Midi GeBAflex-Kit 3.5 kDa MWCO systems (Gene Bio Application Ltd). Then, trypsin (2% w/w from Worthington) treated with TPCK (L-tosyl phenylalanyl chloromethyl ketone) was added and the protein solution was incubated for 4 h at 37°C. The samples were directly analysed in UPLC-MS.

### 2.7. UPLC-MS

Coupled to mass spectrometry detection, separations were performed using Waters Acquity I-Class chromatography system equipped with a C<sub>18</sub> UPLC WATERS Acquity CSH (2.1 x 100 mm, Ø<sub>particles</sub>=1.7μm). The mobile phase eluents used: (A) 0.1% formic acid (v/v) in water and (B) 0.1% formic acid and 90% acetonitrile (v/v/v) in water. Gradient elution for protein digestion coverage was

0-12% of B in 6 min then 12-50% B in 6 min and 50-100% B in 3 min, flow rate 0.5 mL.min<sup>-1</sup>, T<sub>column</sub>=30°C. For dimer identification in KTSLY and digested Δ25-centrin 2, the gradient was: 0% B for 1 min, 0-15% of B in 12 min and then 15-50% B in 3 min, flow rate 0.6 mL.min<sup>-1</sup>, T<sub>column</sub>=20°C (Figures 3 and 5) and flow rate 0.5 mL.min<sup>-1</sup>, T<sub>column</sub>=30°C for the optimized conditions (Figure 6). For tyrosine, the gradient was 0% B for 1 min and 0-10% of B in 10 min, flow rate 0.6 mL.min<sup>-1</sup>, T<sub>column</sub>=30°C. MS experiments were performed on a Q-ToF instrument (SYNAPT G2-Si HDMS, Waters Compagny, Manchester, UK). The instrument was equipped with an ESI (ElectroSpray Ionization) source and was operated in positive ion electrospray ionization mode. The collision gas was Ar. The nebulizer and desolvation gas was N<sub>2</sub>. Calibration was performed using sodium trifluoroacetate between *m/z* 159.016 and *m/z* 1926.317. Operating instrumental parameters were set as follows: capillary voltage 1.2 kV, sampling cone 50 V, source offset 30 V, nebulization gas pressure 4 bar, source temperature 100°C, desolvation temperature 450°C, desolvation gas flow 600 L/h. For MS-MS (Tandem Mass Spectrometry) experiments, trap collision energy was set to 30 eV. No LockSpray was used as internal calibration procedure for these experiments, thus a rather large ± 50 ppm conservative tolerance was used for data interpretation.

### 3. Results

#### 3.1. Oxidative dimerization of a full-length protein and a synthetic peptide

Δ25-centrin 2 samples were irradiated at different doses, from 0 to 40 Gy. In order to compare dimer formation for both radicals (HO• and N<sub>3</sub>•), electrophoresis gel appeared as a suitable technique. For each dose, the same amount of protein was deposited on the gel allowing qualitative and quantitative comparison for both irradiation conditions. In Figure 1A, monomeric form of the protein can be seen just above 15kDa on the gel. HO• oxidation (Figure 1A Left) leads to the formation of higher molecular weight species of the protein (around 37kDa). Previously, we confirmed with mass spectrometry that this band corresponds to a dimer [40, 41]. Also, a lower molecular weight band can be detected just below the monomer that could correspond to the loss of a small protein fragment. In addition to dimerization and backbone cleavage, hydroxyl radicals are also expected to generate many residue oxidations that would not migrate differently from the monomer band as their mass modification is negligible compared to the total protein mass. Indeed, when comparing the monomeric bands from 0 to 35 Gy, these bands seem to become more and more diffuse with the increasing dose, putatively indicating some new oxidized products. On Figure 1A Right, N<sub>3</sub>• oxidation induces exclusively dimers (around 37kDa) and trimers (between 55 and 70kDa).

Though electrophoresis is not a very precise quantitative method, it can be used as a first approach to estimate dimer contents for each type of oxidation. We plotted the intensity of the bands for each well of the gel. First considering azide oxidations and assuming that all the bands observed on the gel represent 100% of the protein deposited, we were able to quantify the dimer formation as a function of

the radical concentration. Figure 1B shows a linear increase of the dimer concentration as a function of  $[N_3^{\cdot}]$  produced by radiolysis, up to ca. 5.6  $\mu\text{M}$  and then a slowdown consistent with the trimer appearance. The slope deduced is  $0.44 \pm 0.02$  which means that each azide radical react to form a protein radical that then dimerize nearly stoichiometrically (~90%). With  $\text{HO}^{\cdot}$ , dimerization is less significant, a dose of 10 Gy corresponding to 5.6  $\mu\text{M}$  of  $\text{HO}^{\cdot}$  leads to ca. 0.9  $\mu\text{M}$  of dimer compared to ca. 2.5  $\mu\text{M}$  for  $N_3^{\cdot}$ .

In addition to electrophoresis, we also performed mass spectrometry experiments after chromatographic separation in order to characterize more precisely the dimer formation. Irradiated samples of  $\Delta 25$ -centrin 2 were analysed by UPLC-MS after tryptic digestion without any sample preparation such as oligomers separation (monomer, dimer, trimer...). According to  $\Delta 25$ -centrin 2 sequence and the fact that trypsin cleaves protein at a lysine or an arginine residue, we can expect two peptides containing the terminal tyrosine, KTLSY and TLSY. Analysis of non-irradiated and digested  $\Delta 25$ -centrin 2 was first performed and separation by liquid chromatography of the cleaved peptides is presented in Figure 2. After optimization of the separation conditions and mass spectra analysis, we identified all the tryptic peptides leading to a full protein coverage. KTLSY peptide has been evidenced as expected and is eluted at 4.65 min, TLSY is eluted at 6.41 min (not shown). As  $^{172}\text{Tyr}$  is known to belong to a flexible part of the protein made of 6 amino acids [44], we wanted to focus on the longer peptide, i.e. KTLSY (168-172) considered as a good model for this flexible region and decided to work on a synthetic peptide build on the same sequence to perform preliminary studies.

Synthetic KTLSY peptide was irradiated at different doses from 0 to 40 Gy with  $\text{HO}^{\cdot}$  and  $N_3^{\cdot}$  and the oxidized mixture was then analysed by UPLC-MS. According to the electrophoresis gels, we were aware that in addition to dimers we can expect trimer formation for the dose range studied. The calculated monoisotopic mass of the dimer formed by a covalent bridge between two KTLSY (named di-KTLSY) peptide is  $m/z$  610.33 (doubly charged). Unfortunately,  $m/z$  610.33 is simultaneously the M+1 isotopic peak of the triply charged trimer. Consequently, in Figure 3 are presented the extracted chromatograms for  $m/z$   $610.00 \pm 0.05$  (monoisotopic peak of the triply charged trimer),  $m/z$   $610.83 \pm 0.05$  (dimer specific) and  $m/z$   $610.33 \pm 0.05$  (dimer and trimer). The first noticeable and unexpected result is that several chromatographic peaks are undoubtedly corresponding to these  $m/z$ : several di-KTLSY and tri-KTLSY seem to be formed under irradiation with azide radical. To ensure that they effectively correspond to di-KTLSY and tri-KTLSY, mass spectra for different retention times were extracted and presented in Figure 4 confirming the dimer/trimer attribution according to their relative charge state and isotopic profile. Thus when relying on accurate mass extracted ion chromatograms, finding the retention times of dimers is best achieved with following  $m/z$  610.83. Figure 5 shows extracted chromatograms of irradiated KTLSY under  $\text{HO}^{\cdot}$  (A) and  $N_3^{\cdot}$  (B) at 0, 10 and 40 Gy. At least five different dimers (named  $D_1$  to  $D_5$ ) can be distinguished from the baseline for both radicals at 10

and 40 Gy with a higher signal to noise ratio for azide radical. Among the five identified dimers, Figure 5 shows that one (D<sub>1</sub>) is formed in a much higher proportion than all the others.

As trimers co-elute with three dimers over five, we decided to improve the separation to better isolate each peak in order to run MS-MS experiments, in order to localize the cross-link formed within the peptides. As Figure 5 shows that HO<sup>•</sup> and N<sub>3</sub><sup>•</sup> radicals form the same peptide dimers, the optimization was only performed with azide which provides a better signal to noise ratio.

By adjusting the column temperature and the flow rate, an optimized separation was obtained for KTSLY irradiated with N<sub>3</sub><sup>•</sup> at 40 Gy: dimers are now isolated from any trimers allowing the  $m/z$  610.33 selection giving a higher intensity (Figure 6A) and then to perform more specific fragmentation. MS-MS of all the dimers (D<sub>1</sub> to D<sub>5</sub>) show the same fragmentation pattern, measured  $m/z$  are gathered in Table 1. The MS-MS fragmentation spectrum obtained for the most intense peak for N<sub>3</sub><sup>•</sup> oxidation (di-KTSLY D<sub>1</sub> retention time 7.96 min) is presented in Figure 7. The fragmentation leads to  $\gamma$  fragments series on both sides of the di-tyrosine bridge, including many fragmentations on both side. The presence of these series shows all characteristics of a dimer formed by a di-tyrosine bridge: fragmentation of all amide bonds down to Y-Y were observed. The latter is the most abundant one, at  $m/z$  361.16 and is observed for all five peaks, confirming that oxidation of the peptide leads to the formation of five isomeric di-KTSLY that are covalently bound through their terminal tyrosinyl residue.

As five di-KTSLY were highlighted for the synthetic peptide, we can wonder if full length protein behaves the same. After oxidation by HO<sup>•</sup> or N<sub>3</sub><sup>•</sup> (40 Gy) and tryptic digestion of  $\Delta$ 25-centrin 2, we searched for species at  $m/z$  610.33 as in the synthetic KTSLY. From Figure 6 A) and B), it is obvious that with azide radical, the synthetic peptide and the protein have the same dimerization behaviour considering the number of dimers, their retention times and intensity profiles. Then they can be considered as equivalent species which legitimates the in-depth study of synthetic KTSLY. For HO<sup>•</sup> which exhibits a chromatogram with a lower signal to noise ratio than N<sub>3</sub><sup>•</sup>, only four dimers (D<sub>1</sub> to D<sub>4</sub>) can be distinguished from the baseline. Measured  $m/z$  ratios and their corresponding charge state confirm that each peak corresponds to two KTSLY peptides linked by a covalent bond (Table 2).

### 3.2. Tyrosine oxidation

In order to study more precisely the dimerization process occurring with the protein and the peptide, we compared it to a simpler system i.e. the free amino acid, already much better studied in the literature. As for the other samples, tyrosine was irradiated at different doses, from 0 to 40 Gy. As electrophoresis is not suitable for a small system, only UPLC-MS analysis was performed to identify the chemical modifications induced. Figure 8 shows the comparison of HO<sup>•</sup> and N<sub>3</sub><sup>•</sup> oxidation at 0 and 40 Gy. Though the non-irradiated sample exhibits only one peak corresponding to non-modified Tyr ( $m/z$  182.086, not shown), our chromatographic conditions allowed us to separate several peaks

(Figure 8) after irradiation. Chromatograms presented in Figure 8 only bring to light chromatographic peaks containing species with  $m/z$  361.139 which corresponds to the calculated mass of a dimer of tyrosine formed through a covalent bond. At 40 Gy, chromatogram B) enables to distinguish four peaks at retention times 2.15, 3.89, 4.09 and 4.38 min responding to di-tyrosine  $m/z$  ratio. To confirm di-tyrosine bridge formation, we extracted the mass spectra for these retention times (Figure 9). The main peak found at  $m/z$  361.136 confirms the formation of four different covalent dimers. In terms of intensity, the peak at 2.15 min is present in higher abundance compared to the two others. Hydroxyl dimerization pattern appears very similar to that of azide as in chromatogram C) four peaks are also identified with very similar retention times: 2.15, 3.91, 4.11 and 4.40 min for  $m/z$  361.14. Their corresponding extracted mass spectrum show the same pattern (data not shown) and confirm as for azide the presence of four di-tyrosine bridges. In addition to dimers,  $\text{HO}^\bullet$  but not  $\text{N}_3^\bullet$  leads to additional oxidative process on the sample. As it is well-known,  $\text{HO}^\bullet$  can add to the ring to form OH-adducts. Oxidative products corresponding to simple ( $m/z$  198.07) and double ( $m/z$  214.07) OH-addition to the ring were actually identified.

#### 4. Discussion

Hydroxyl and azide oxidation behaviours were studied and compared through three different systems: simple tyrosine, a five amino acid peptide (KTSLY) and a protein  $\Delta 25$ -centrin 2 both containing a C-terminal tyrosine. For each of the systems considered, it is clear from our data that several and identical dimers are formed for both hydroxyl and azide radicals.

Azide oxidation of the protein leads to the formation of five dimers. Due to an insufficient signal/noise ratio on the digested protein mixture chromatogram, we only detect four dimers for  $\text{HO}^\bullet$ , characterized by the same retention times as for azide. Additional oxidations are expected and were observed for hydroxyl radicals. However, based on the chromatograms and the relative dimer peak intensities observed, we consider that  $\text{HO}^\bullet$  and  $\text{N}_3^\bullet$  induce similar dimerization i.e. five dimers of  $\Delta 25$ -centrin 2.

As hydroxyl radicals are known to exhibit poor selectivity, one could expect that dimerization occurs *via* side-chain and backbone links along the entire sequence. Nevertheless, after careful analysis of our UPLC-MS-MS experiments we can conclude that, both for the peptide or for the protein, oxidative dimerization leads to the formation of five different species all covalently linked by their terminal Tyr residues. To ensure the biological relevance of these dimerizations, samples were also irradiated at 37°C and exhibit exactly the same oxidative dimerization (not shown).

Whatever the peptide, synthetic or arising from protein digestion, respective chromatographic peaks display the same retention time and patterns are identical. This demonstrates that this small peptide mimics quite precisely the protein dimerization. The five-residue peptide exhibits no structured conformation in circular dichroism (not shown) and  $\Delta 25$ -centrin 2 is known to be structured with

mainly alpha helices except for its C-terminal part where at least 6 residues are in a very flexible region [44]. Flexibility and accessibility of the Tyr residue could be responsible for so many dimers, corroborating a similar behaviour for both the peptide and the protein. Protein oxidative pattern is expected to be governed by residue accessibility, which is the basis for its use as a method to map protein-protein interactions [45]. Nevertheless, for tyrosine alone only four dimers were clearly evidenced. Here also, such a higher dimer number was never reported before.

From the literature and Tyr oxidation mechanisms described, it is not so unexpected to form at least two tyrosine dimers [46]. For example, Fonseca et al. proposed the presence of different isomers for a dipeptide [47]. Also, dimer formations are the result of recombination of different intermediate radicals generated during oxidation process. In the case of  $N_3^*$ , only an electron transfer is supposed to occur leading to an oxygen-centered radical and no  $N_3^*$  addition on the ring was reported. Though this radical is mainly localized on the oxygen atom, the most encountered dimer in the literature is bridged through two carbons from the ring (*ortho-ortho* dimer, Scheme 1). Its structure was elucidated by NMR (Nuclear Magnetic Resonance) or mass spectrometry performed after isotopic substitution [33, 40]. This dimer formation arises from the reaction between two carbon-centered radicals, which can be explained by the electron density of  $TyrO^*$ , delocalized on the *ortho* and *para* positions (Scheme 2) [48]. Yamamoto and Okuda in 1975 [29] suggested another structure named *iso* di-tyrosine (Scheme 1) resulting from covalent bonding between  $TyrO^*$  **1** and Tyr (*C'-ortho*) **2** which was later identified in 1984 by Karam et al. after radiolytic oxidation [12]. *Iso* di-tyrosine was also identified in plant cell-wall glycoproteins [31]. Additional dimers that we evidence here for  $\Delta 25$ -centrin 2 could be the result of the recombination between different radicals formed within electronic delocalization of  $TyrO^*$ . In the case of cresol the dimer formed between the *C-para* (equivalent structure **3** Scheme 2) and phenoxyl (equivalent structure **1** Scheme 2) radicals seems to be one of the most stable species [13], then if Tyr behaves as cresol a third dimer could correspond to the recombination of **1** and **3**. Also, as the peptide exhibits an additional dimer compared to tyrosine, the only difference between both species being the  $NH_3^+$  terminal group, this suggests that the NH amide function is important for the formation of at least one dimer.

In this study, we also show that among the dimers formed, one has a much higher yield of formation than the others. Previously, we performed azide oxidation of deuterated tyrosine in *ortho* position followed by HPLC separation [40]. Due to much lower resolution for the chromatographic separation, we only evidenced one dimer that was collected for mass analysis. Our results showed that this chromatographic peak was mainly made of *ortho-ortho* dimer. Considering that we had a mixture of all the dimers now evidenced, we can assume that the *ortho-ortho* represents the main dimerization product. Nevertheless, a precise structure elucidation of all these protein dimers is further necessary.

According to previous pulse radiolysis studies [49], HO• was shown to react with tyrosine through different pathways. It can react by hydrogen abstraction on the hydroxyl function but also by addition on the ring. Solar et al. identified, based on their absorption properties, 4 tyrosine radicals, Tyr•(OH) which is a carbon-centered radical after addition of HO• in *ortho* or *meta* ring position on the aromatic cycle, Tyr•(CH) a carbon-centered radical on CH<sub>2</sub> group after abstraction of H by HO• and TyrO• corresponding to the phenoxyl radical (Scheme 2). As for HO• and N<sub>3</sub>• radicals, we identified the same dimers, they should originate from a common pathway. Then, we suggest they all arise from TyrO• and its mesomers. Also, Gmeiner and Seelos showed that blocking of the phenolic position of the tyrosine by a phosphate moiety abolishes tyrosine fluorescent dimerization[50] when oxidation is performed by the reaction between horseradish peroxidase (HRP) and H<sub>2</sub>O<sub>2</sub>. This strengthens the hypothesis that TyrO• is the main precursor of the dimerization process. Hydroxyl radical's addition to the ring is responsible for other types of oxidation of tyrosine as addition of oxygen atoms on the ring to form DOPA for example. Therefore, azide oxidation can be a preferred tool to study protein dimerization as it mimics the *in vivo* oxidative process.

Also, we show that for both radicals protein dimerization appears as the predominant oxidation consequence. In the present study, we used two different approaches to estimate dimer proportions formed for both hydroxyl and azide, i.e. electrophoresis and mass spectrometry. According to electrophoresis gels analysis, we estimate that for Δ25-centrin 2, dimerization is a major product with both radicals. Dimer formation is nearly stoichiometric with azide as 10 Gy corresponding to 5.6 μM of N<sub>3</sub>• leads to 2.5 μM of dimer. This yield of formation is lowered with hydroxyl radicals as we obtained a ratio dimer<sub>[HO•]</sub>:dimer<sub>[N<sub>3</sub>•]</sub> of 1:3. In other words, 5.6 μM of HO• radicals generates ca. 0.9 μM of centrin dimer. This means that a third of the HO• formed in solution by water radiolysis are scavenged by the only Tyr residue to generate dimers. Aware that gel analysis only gives an estimation of dimerization and in order to strengthen the reliability of this comparison, we integrated dimer peaks areas detected with mass spectrometry. Here also, considering areas of the most intense dimer, dimer<sub>[HO•]</sub>:dimer<sub>[N<sub>3</sub>•]</sub> ratio is found to be 35%. These two approaches give the same dimer proportion, thus demonstrating the predominance of dimerization process both for N<sub>3</sub>• and HO• centrin oxidation. Based on its redox potential, azide is expected to first react on Trp residues and then on Tyr. It was also shown to be able to oxidize methionine which redox potential is lowered under specific conditions [36, 37]. Δ25-centrin 2 does not possess any Trp and has only one terminal tyrosine located in a very flexible region. These protein properties seem to be responsible for a stoichiometric induced dimerization. As for hydroxyl radical, its redox potential is about 2.3 V, any residue in these 148 amino acids sequence could be the target of HO• which should lower drastically the proportion of dimer formed. Nevertheless, we determined that dimerization scavenges ca. 35 % of the hydroxyl radicals, which is a very high proportion. Comparing Δ25-centrin 2 dimerization to other proteins oxidized by N<sub>3</sub>• and HO•, it clearly appears that much higher doses or radical concentrations are often

needed to induce significant tyrosine dimerization. Indeed, considering lysozymes [51] or thioredoxin [52], up to thousands of Gy corresponding to several hundreds of  $\mu\text{M}$  of radicals were necessary to evidence small quantities of dimers. Therefore, we confirm that  $\Delta 25$ -centrin 2 as human centrin 2 [40] can be considered as a very efficient radical scavenger, precursor of dimers.

## 5. Conclusions

From this study, we evidenced that dimerization is the major oxidation induced on  $\Delta 25$ -centrin 2. Also, our UPLC-MS conditions enabled, for the first time, to bring to light at least five di-tyrosine bridges in the case of a protein and a peptide, and four tyrosine dimers for the amino acid after radiolytic oxidation by  $\text{HO}^\bullet$  and  $\text{N}_3^\bullet$ . These results are crucial as tyrosine dimerization is a major oxidative damage induced *in vivo*. Considering that these different dimers could be generated *in vivo*, some questions can be raised. First, since di-tyrosine bridges were evidenced in many pathological cases, the existence of different dimers raises the question of their specific role, consequence or toxicity *in vivo*. Second, di-tyrosine bridges are often used as biomarkers. Some biological tests are based on di-tyrosine detection using commercial antibodies, fluorescent measurements or chromatographic analysis. This raises a question about the specificity of antibodies since immunogen are generated with synthetic *ortho-ortho* di-tyrosine that could not be representative of all the dimers which could be found *in vivo*. Considering fluorescence detection, different dimer structures could be responsible for different fluorescent properties. It is then necessary to ensure that all dimers can undoubtedly be detected. Their detection and separation in biological samples present a real analytical challenge but is a requirement, as their structure elucidation, considering their crucial role in oxidative stress.

## References

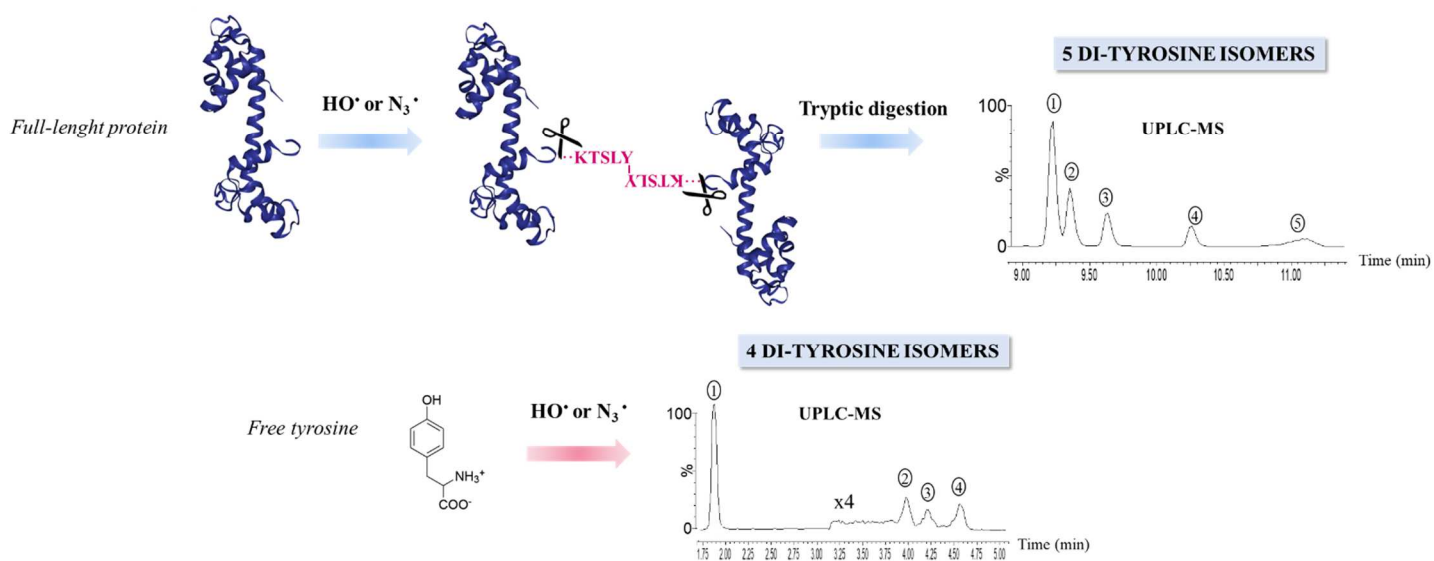
1. Davies, M.J. and R.T. Dean, *Radical-mediated protein oxidation : from chemistry to medicine*. 1997, Oxford; New York: Oxford University Press.
2. Buxton, G.V., et al., *Critical Review of rate constants for reactions of hydrated electrons, hydrogen atoms and hydroxyl radicals ( $\cdot\text{OH}/\cdot\text{O}$  in Aqueous Solution*. Journal of Physical and Chemical Reference Data, 1988. **17**(2): p. 513-886.
3. Aeschbach, R., R. Amado, and H. Neukom, *Formation of dityrosine cross-links in proteins by oxidation of tyrosine residues*. Biochim Biophys Acta, 1976. **439**(2): p. 292-301.
4. Correia, M., et al., *UV-light exposure of insulin: pharmaceutical implications upon covalent insulin dityrosine dimerization and disulphide bond photolysis*. PLoS One, 2012. **7**(12): p. e50733.
5. Degendorfer, G., et al., *Exposure of tropoelastin to peroxyntrous acid gives high yields of nitrated tyrosine residues, di-tyrosine cross-links and altered protein structure and function*. Free Radic Biol Med, 2018. **115**: p. 219-231.
6. Fuentes-Lemus, E., et al., *Binding of rose bengal to lysozyme modulates photooxidation and cross-linking reactions involving tyrosine and tryptophan*. Free Radic Biol Med, 2019. **143**: p. 375-386.
7. Fuentes-Lemus, E., et al., *Photo-oxidation of lysozyme triggered by riboflavin is O<sub>2</sub>-dependent, occurs via mixed type 1 and type 2 pathways, and results in inactivation, site-specific damage and intra- and inter-molecular crosslinks*. Free Radic Biol Med, 2020. **152**: p. 61-73.
8. Fuentes-Lemus, E., et al., *alpha- and beta-casein aggregation induced by riboflavin-sensitized photo-oxidation occurs via di-tyrosine cross-links and is oxygen concentration dependent*. Food Chem, 2018. **256**: p. 119-128.
9. Lehrer, S.S. and G.D. Fasman, *Ultraviolet irradiation effects in poly-L-tyrosine and model compounds. Identification of bityrosine as a photoproduct*. Biochemistry, 1967. **6**(3): p. 757-67.
10. Boguta, G. and A.M. Danciewicz, *Radiation-induced dimerization of tyrosine and glycytyrosine in aqueous solutions*. Int J Radiat Biol Relat Stud Phys Chem Med, 1981. **39**(2): p. 163-74.
11. Getoff, N., *Pulse radiolysis of aromatic amino acids - State of the art*. Amino Acids, 1992. **2**(3): p. 195-214.
12. Karam, L.R., M. Dizdaroglu, and M.G. Simic, *OH radical-induced products of tyrosine peptides*. Int J Radiat Biol Relat Stud Phys Chem Med, 1984. **46**(6): p. 715-24.
13. Shamovsky, I.L., R.J. Riopelle, and G.M. Ross, *Ab Initio Studies on the Mechanism of Tyrosine Coupling*. The Journal of Physical Chemistry A, 2001. **105**(6): p. 1061-1070.
14. Houee-Levin, C., et al., *Exploring oxidative modifications of tyrosine: an update on mechanisms of formation, advances in analysis and biological consequences*. Free Radic Res, 2015. **49**(4): p. 347-73.
15. Malencik, D.A. and S.R. Anderson, *Dityrosine as a product of oxidative stress and fluorescent probe*. Amino Acids, 2003. **25**(3-4): p. 233-47.
16. Mukherjee, S., et al., *Characterization and Identification of Dityrosine Cross-Linked Peptides Using Tandem Mass Spectrometry*. Anal Chem, 2017. **89**(11): p. 6136-6145.
17. Reid, L.O., et al., *Photochemistry of tyrosine dimer: when an oxidative lesion of proteins is able to photoinduce further damage*. Photochem Photobiol Sci, 2019. **18**(7): p. 1732-1741.
18. Kungl, A.J., et al., *Time-resolved fluorescence studies of dityrosine in the outer layer of intact yeast ascospores*. Biophys J, 1994. **67**(1): p. 309-17.
19. Feeney, M.B. and C. Schoneich, *Tyrosine modifications in aging*. Antioxid Redox Signal, 2012. **17**(11): p. 1571-9.
20. Grune, T., *Oxidized protein aggregates: Formation and biological effects*. Free Radic Biol Med, 2020. **150**: p. 120-124.
21. Dalle-Donne, I., et al., *Proteins as biomarkers of oxidative/nitrosative stress in diseases: The contribution of redox proteomics*. Mass Spectrometry Reviews, 2005. **24**: p. 55.

22. Davies, M.J., et al., *Stable markers of oxidant damage to proteins and their application in the study of human disease*. Free Radical Biology and Medicine, 1999. **27**(11): p. 1151-1163.
23. DiMarco, T. and C. Giulivi, *Current analytical methods for the detection of dityrosine, a biomarker of oxidative stress, in biological samples*. Mass Spectrom Rev, 2007. **26**(1): p. 108-20.
24. Al-Hilaly, Y.K., et al., *The involvement of dityrosine crosslinking in alpha-synuclein assembly and deposition in Lewy Bodies in Parkinson's disease*. Sci Rep, 2016. **6**: p. 39171.
25. Al-Hilaly, Y.K., et al., *A central role for dityrosine crosslinking of Amyloid-beta in Alzheimer's disease*. Acta Neuropathol Commun, 2013. **1**: p. 83.
26. Chen, Z., et al., *Characterisation and quantification of protein oxidative modifications and amino acid racemisation in powdered infant milk formula*. Free Radical Research, 2019. **53**(1): p. 68-81.
27. Colombo, G., et al., *A central role for intermolecular dityrosine cross-linking of fibrinogen in high molecular weight advanced oxidation protein product (AOPP) formation*. Biochim Biophys Acta, 2015. **1850**(1): p. 1-12.
28. Zamora, R.A., et al., *Free radicals derived from gamma-radiolysis of water and AAPH thermolysis mediate oxidative crosslinking of eGFP involving Tyr-Tyr and Tyr-Cys bonds: the fluorescence of the protein is conserved only towards peroxy radicals*. Free Radic Biol Med, 2020. **150**: p. 40-52.
29. Yamamoto, O. and A. Okuda, *Radiation-induced binding of OH-substituted aromatic amino acids, tyrosine and dopa, mutually and with albumin in aqueous solution*. Radiat Res, 1975. **61**(2): p. 251-60.
30. Shen, H.-R., et al., *Photodynamic cross-linking of proteins: V. Nature of the tyrosine-tyrosine bonds formed in the FMN-sensitized intermolecular cross-linking of N-acetyl-L-tyrosine*. Journal of Photochemistry and Photobiology A: Chemistry, 2000. **133**(1): p. 115-122.
31. Fry, S.C., *Isodityrosine, a new cross-linking amino acid from plant cell-wall glycoprotein*. Biochem J, 1982. **204**(2): p. 449-55.
32. Brady, J.F., I.H. Sadler, and S.C. Fry, *Di-isodityrosine, a novel tetrameric derivative of tyrosine in plant cell wall proteins : a new potential cross-link*. Biochem. J., 1996. **315**: p. 323-327.
33. Jacob, J.S., et al., *Human phagocytes employ the myeloperoxidase-hydrogen peroxide system to synthesize dityrosine, trityrosine, pulcherosine, and isodityrosine by a tyrosyl radical-dependent pathway*. J Biol Chem, 1996. **271**(33): p. 19950-6.
34. Hagglund, P., M. Mariotti, and M.J. Davies, *Identification and characterization of protein cross-links induced by oxidative reactions*. Expert Rev Proteomics, 2018. **15**(8): p. 665-681.
35. Grune, T., B. Catalgol, and T. Jung, *Oxidative Stress and Protein Oxidation*, in *Protein Oxidation and Aging*, W.O. Books, Editor. 2012. p. 1-214.
36. Brunelle, P. and A. Rauk, *One-Electron Oxidation of Methionine in Peptide Environments: The Effect of Three-Electron Bonding on the Reduction Potential of the Radical Cation*. The Journal of Physical Chemistry A, 2004. **108**(50): p. 11032-11041.
37. Kadlcik, V., et al., *Reductive Modification of a Methionine Residue in the Amyloid-β Peptide*. Angewandte Chemie International Edition, 2006. **45**(16): p. 2595-2598.
38. Araki, M., et al., *Centrosome protein centrin 2/caltractin 1 is part of the xeroderma pigmentosum group C complex that initiates global genome nucleotide excision repair*. J Biol Chem, 2001. **276**(22): p. 18665-72.
39. Lutz, W., et al., *Phosphorylation of centrin during the cell cycle and its role in centriole separation preceding centrosome duplication*. J Biol Chem, 2001. **276**(23): p. 20774-80.
40. Blouquit, Y., et al., *High sensitivity of human centrin 2 toward radiolytical oxidation: C-terminal tyrosinyl residue as the main target*. Free Radic Biol Med, 2007. **43**(2): p. 216-28.
41. Brun, E., et al., *Oxidative stress induces mainly human centrin 2 polymerisation*. Int J Radiat Biol, 2010. **86**(8): p. 657-68.
42. Tourbez, M., et al., *Calcium-dependent self-assembly of human centrin 2*. J Biol Chem, 2004. **279**(46): p. 47672-80.
43. Spinks, J.W.T. and R.J. Woods, *An Introduction to Radiation Chemistry; 3rd ed.; Wiley-Interscience publication: New York, USA. 1990.*

44. Matei, E., et al., *C-terminal half of human centrin 2 behaves like a regulatory EF-hand domain*. *Biochemistry*, 2003. **42**(6): p. 1439-50.
45. Xu, G. and M.R. Chance, *Hydroxyl radical-mediated modification of proteins as probes for structural proteomics*. *Chem Rev*, 2007. **107**(8): p. 3514-43.
46. Eickhoff, H., G. Jung, and A. Rieker, *Oxidative phenol coupling—tyrosine dimers and libraries containing tyrosyl peptide dimers*. *Tetrahedron*, 2001. **57**(2): p. 353-364.
47. Fonseca, C., et al., *Reactivity of Tyr-Leu and Leu-Tyr dipeptides: identification of oxidation products by liquid chromatography-tandem mass spectrometry*. *J Mass Spectrom*, 2009. **44**(5): p. 681-93.
48. Sjoberg, B.M., et al., *The tyrosine free radical in ribonucleotide reductase from Escherichia coli*. *J Biol Chem*, 1978. **253**(19): p. 6863-5.
49. Solar, S., W. Solar, and N. Getoff, *Reactivity of hydroxyl with tyrosine in aqueous solution studied by pulse radiolysis*. *The Journal of Physical Chemistry*, 1984. **88**(10): p. 2091-2095.
50. Gmeiner, B. and C. Seelos, *Phosphorylation of tyrosine prevents dityrosine formation in vitro*. *FEBS Lett*, 1989. **255**(2): p. 395-7.
51. Stuart-Audette, M., et al., *Re-evaluation of intramolecular long-range electron transfer between tyrosine and tryptophan in lysozymes. Evidence for the participation of other residues*. *Eur J Biochem*, 2003. **270**(17): p. 3565-71.
52. Sicard-Roselli, C., et al., *Thioredoxin Ch1 of Chlamydomonas reinhardtii displays an unusual resistance toward one-electron oxidation*. *Eur J Biochem*, 2004. **271**(17): p. 3481-7.

# GRAPHICAL ABSTRACT

## Highlight of several di-tyrosine bridge isomers



## Highlights

- UPLC-MS optimized separation highlights new additional di-tyrosine bridges induced by hydroxyle or azide radicals
- Oxidative radicals ( $\text{HO}^\bullet$  or  $\text{N}_3^\bullet$ ) produced by gamma radiolysis lead to five di-tyrosine bridges in a full-length protein ( $\Delta 25$ -centrin 2)
- At least four covalent dimers of the tyrosine amino acid are formed under the effect of oxidizing radicals

# FIGURE 1

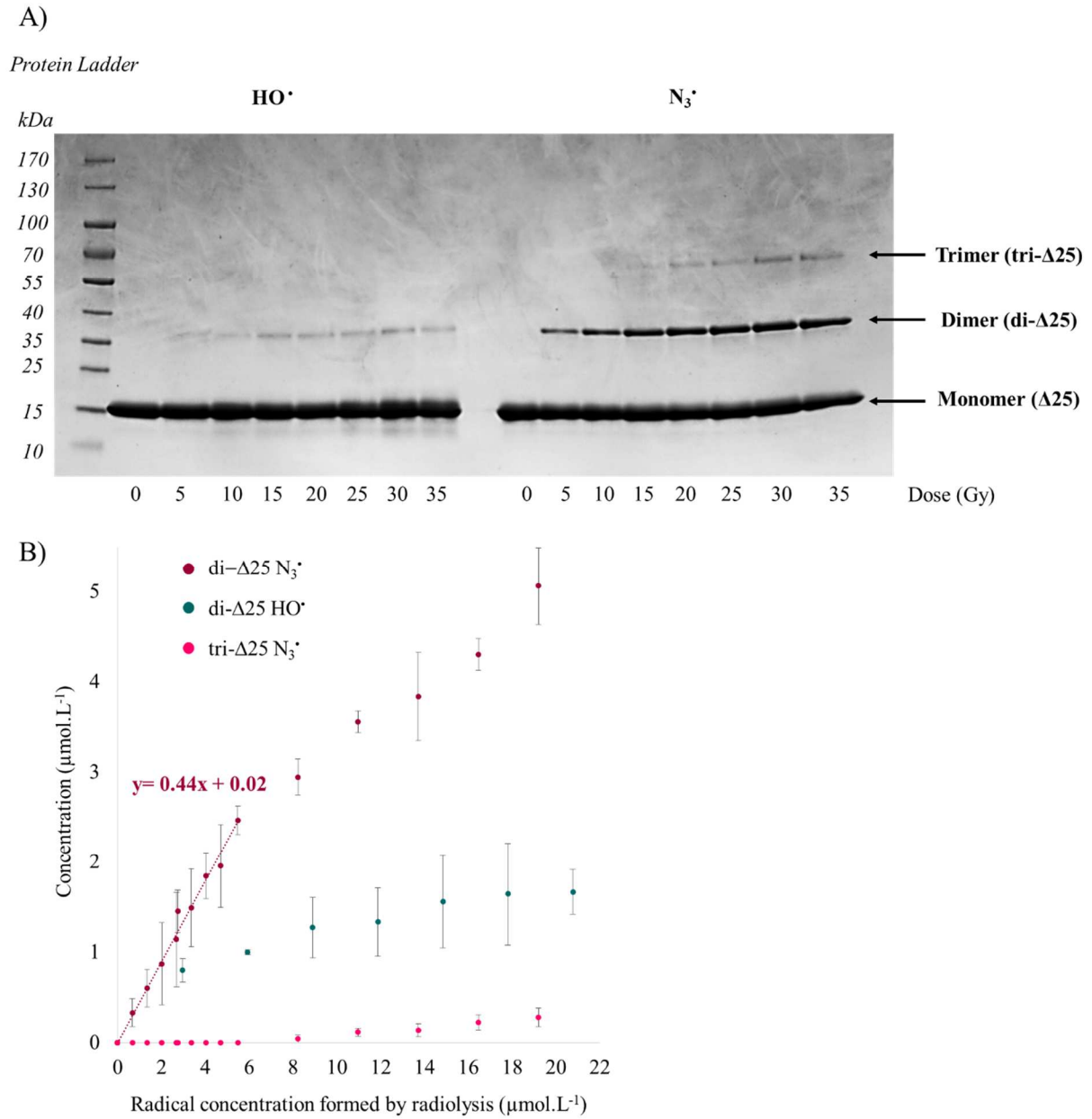


Figure 1: A) Electrophoresis gel profile obtained after radiolytic oxidation by HO<sup>•</sup> (Left) and N<sub>3</sub><sup>•</sup> (Right) of Δ25-centrin 2 with increasing doses in the absence of oxygen. B) Δ25 dimer and trimer concentration evolution with increasing concentrations of HO<sup>•</sup> and N<sub>3</sub><sup>•</sup> produced by radiolysis. Each point is the average of three independent analysis of three different gels. Linear regression was carried out until 5.6 μM of azide radical as trimer is detected from this dose.

# FIGURE 2

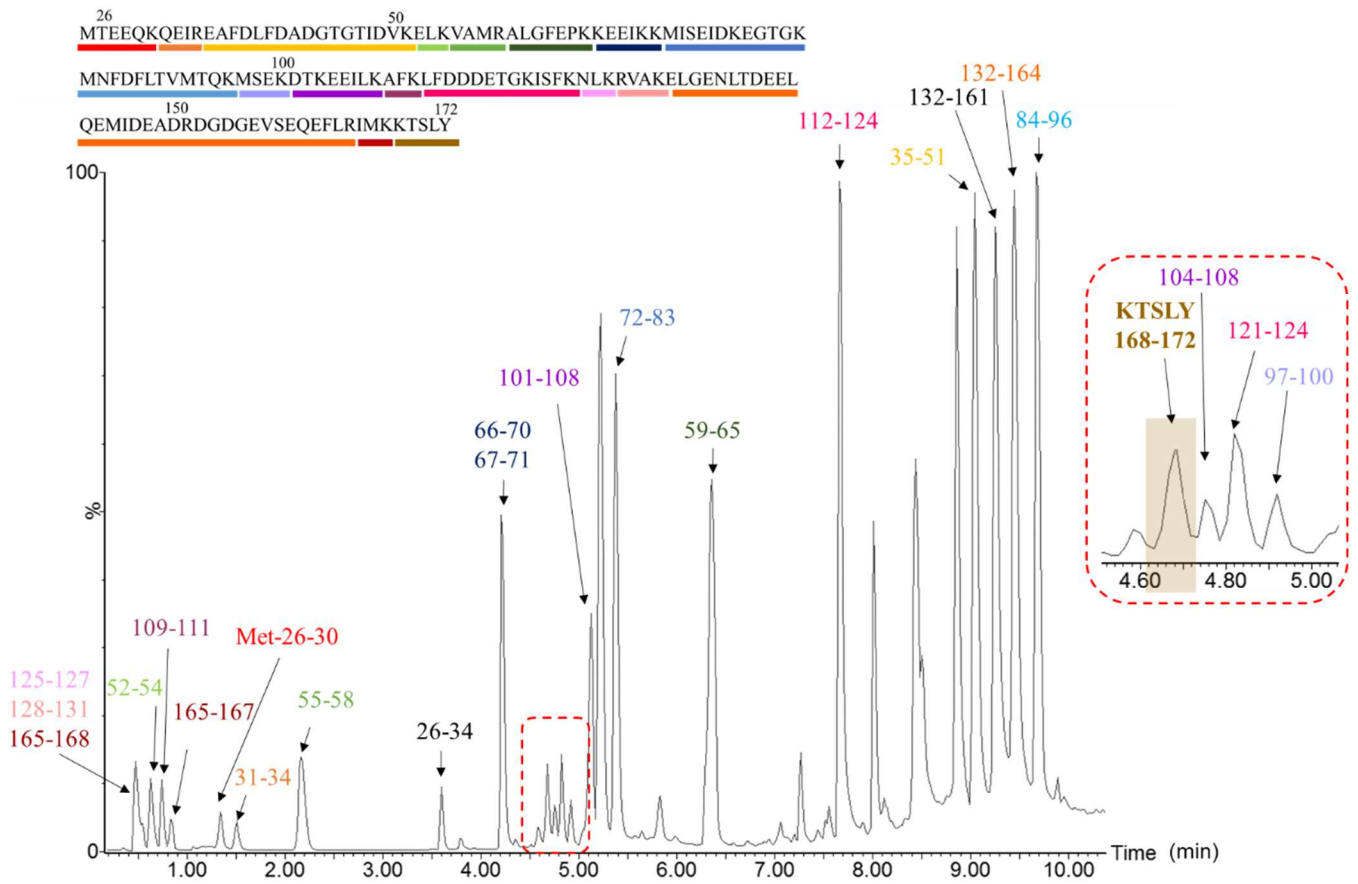


Figure 2: Chromatogram of non-irradiated  $\Delta 25$ -centrin 2 tryptic digestion. Each tryptic peptide is represented by a colour in the sequence and on the chromatogram. The insert corresponds to a zoom of KTSLY peptide.

# FIGURE 3

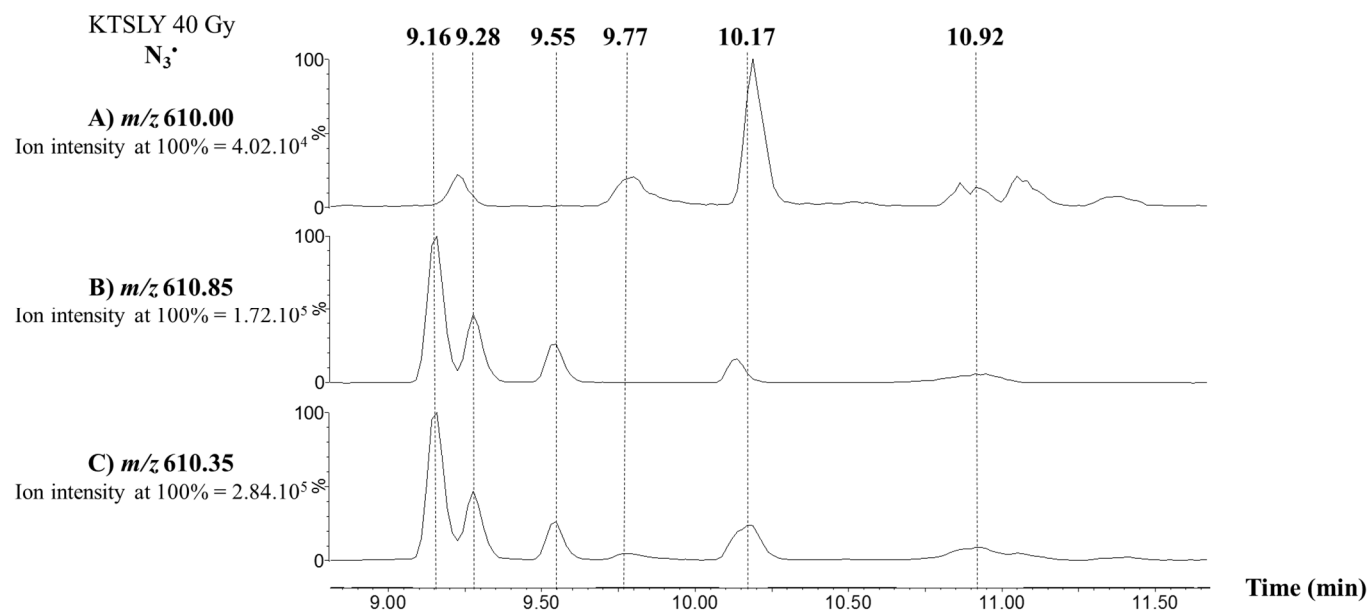


Figure 3: Extracted ion chromatograms of irradiated KTSLY at 40 Gy in  $N_3^+$  production conditions for A)  $m/z$   $610.000 \pm 0.05$ ; B)  $m/z$   $610.85 \pm 0.05$  and C)  $m/z$   $610.35 \pm 0.05$ .

# FIGURE 4

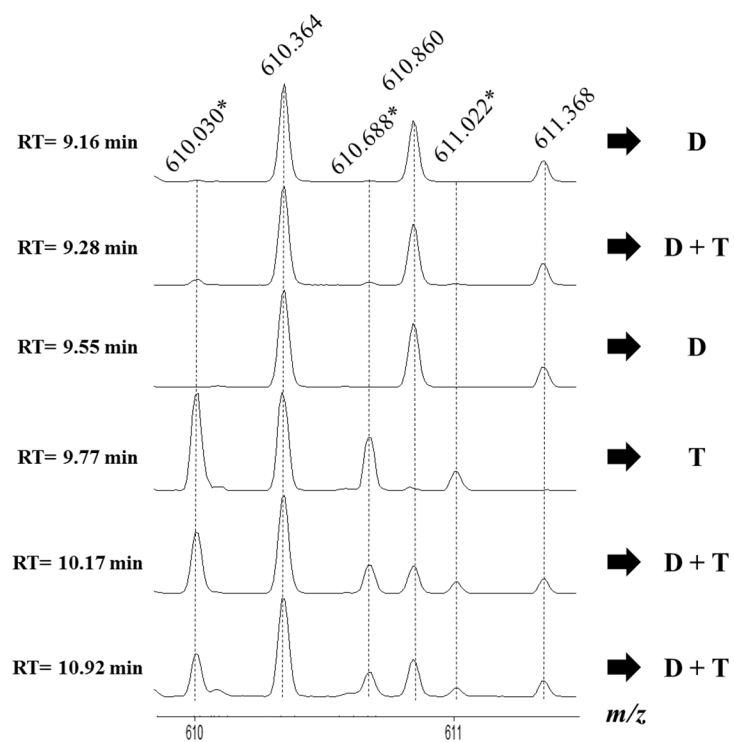


Figure 4: Full scan MS spectra extracted from Figure 3 (KTSLYN<sub>3</sub> 40Gy) at different retention times:  $m/z$  ratio identified by a star correspond to trimer contribution only. D: dimer. T: trimer.

## FIGURE 5

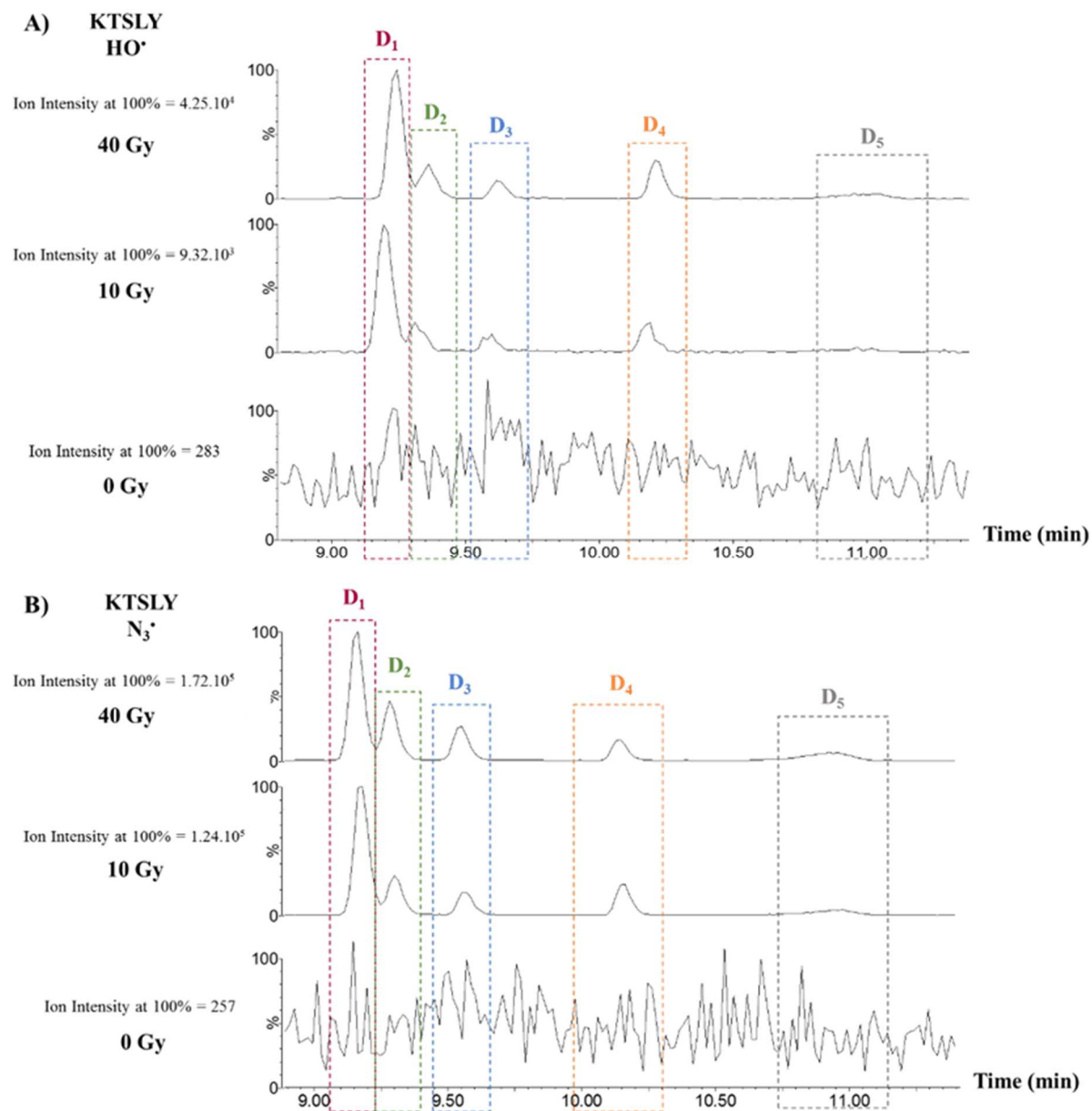


Figure 5: Extracted ion chromatograms ( $m/z$   $610.85 \pm 0.05$ ) for irradiated KTSLY at 40, 10 and 0 Gy under: A) HO<sup>•</sup> reaction conditions; B) N<sub>3</sub><sup>•+</sup> reaction conditions.

**FIGURE 6**

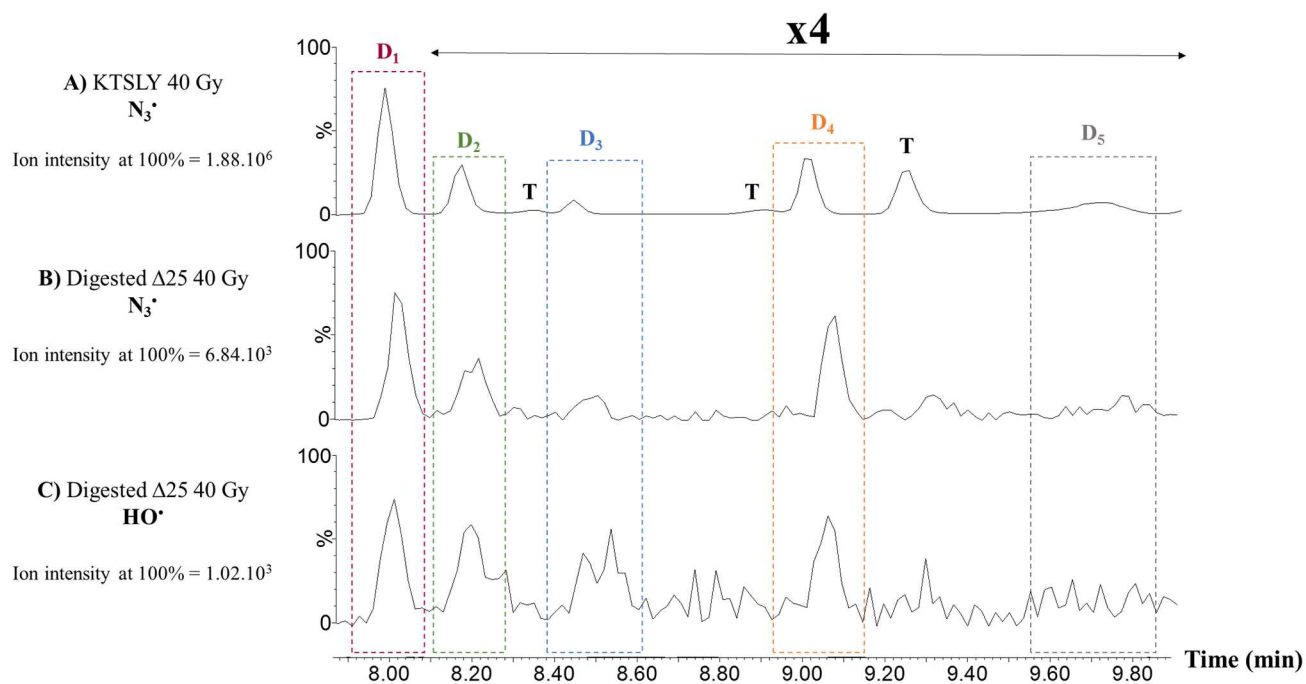


Figure 6: Extracted ion chromatograms ( $m/z$  610.35  $\pm$  0.05) for A) KTSLY irradiated with  $N_3^\bullet$  at 40 Gy; B) Digested  $\Delta 25$  irradiated with  $N_3^\bullet$  at 40 Gy; C) Gy Digested  $\Delta 25$  irradiated with  $HO^\bullet$  at 40 Gy.

# FIGURE 7

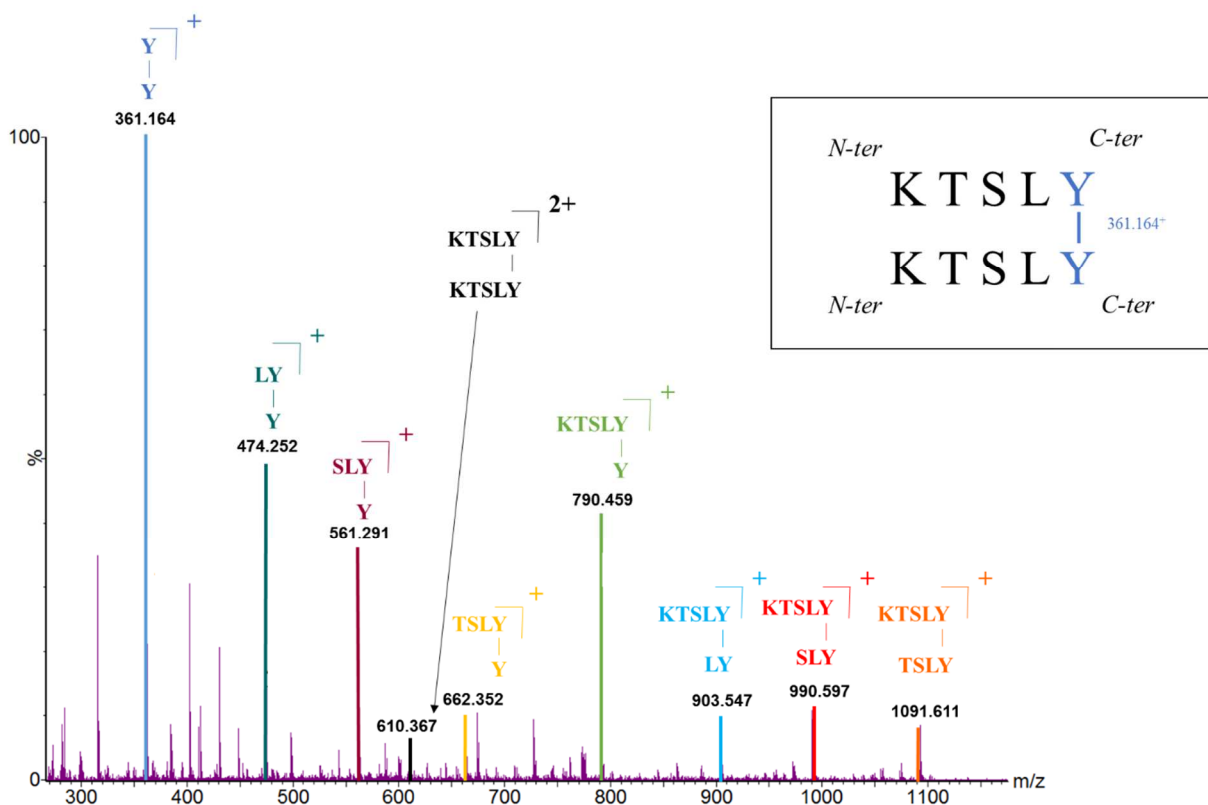


Figure 7: Fragmentation mass spectrum (MS-MS) of di-KTSLY D<sub>1</sub> (retention time=7.96 min) irradiated at 40 Gy with N<sub>3</sub><sup>+</sup> at precursor m/z 610 ± 1. The insert is a representation of the di-tyrosine bridge formed between two KTSLY peptides. The most intense peak at m/z 361.16 is represented in dark blue.

# FIGURE 8

Ion intensity at 100% is fixed at  $8.00 \cdot 10^4$

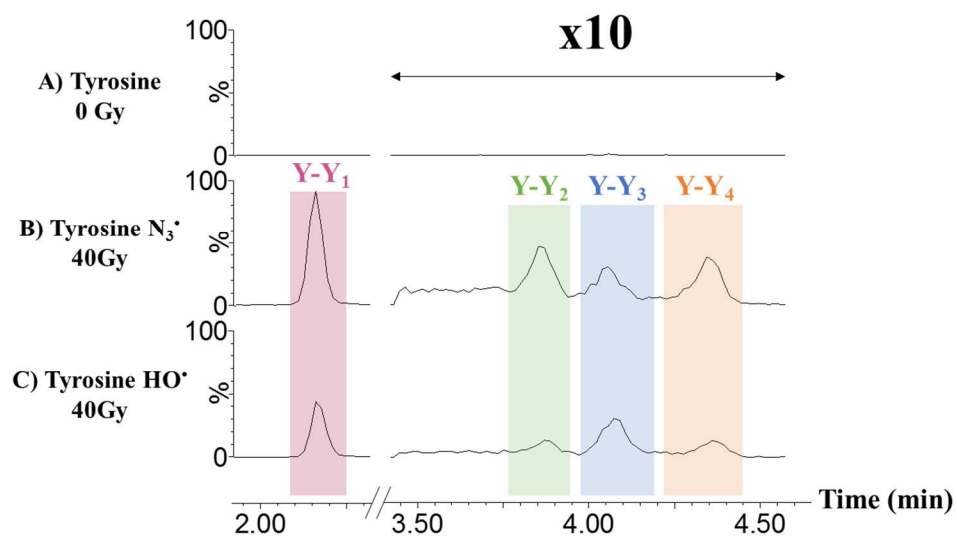


Figure 8: Extracted ion chromatograms of irradiated tyrosine under  $HO^\bullet$  and  $N_3^\bullet$  for  $m/z 361.13 \pm 0.05$  (di-tyrosine): A) Non irradiated; B)  $N_3^\bullet$  condition, 40 Gy irradiation; C)  $HO^\bullet$  condition, 40 Gy irradiation.

# FIGURE 9

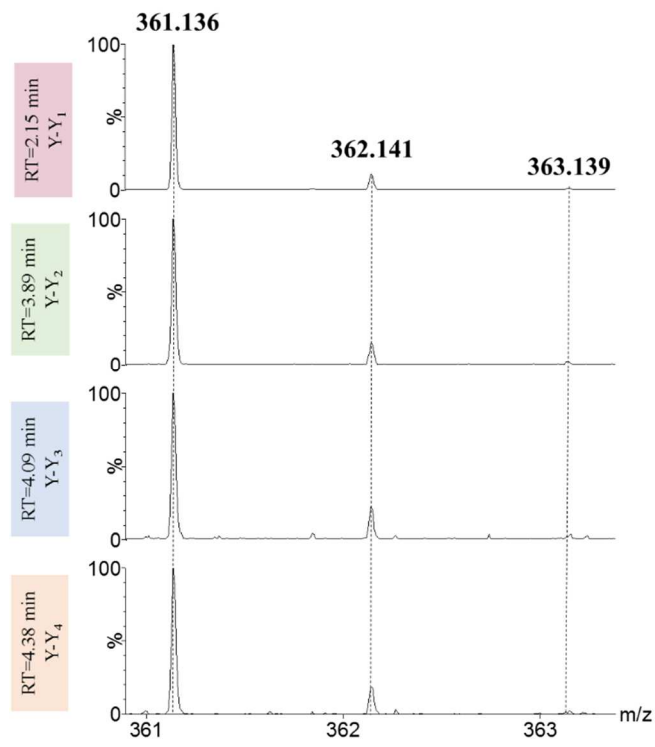
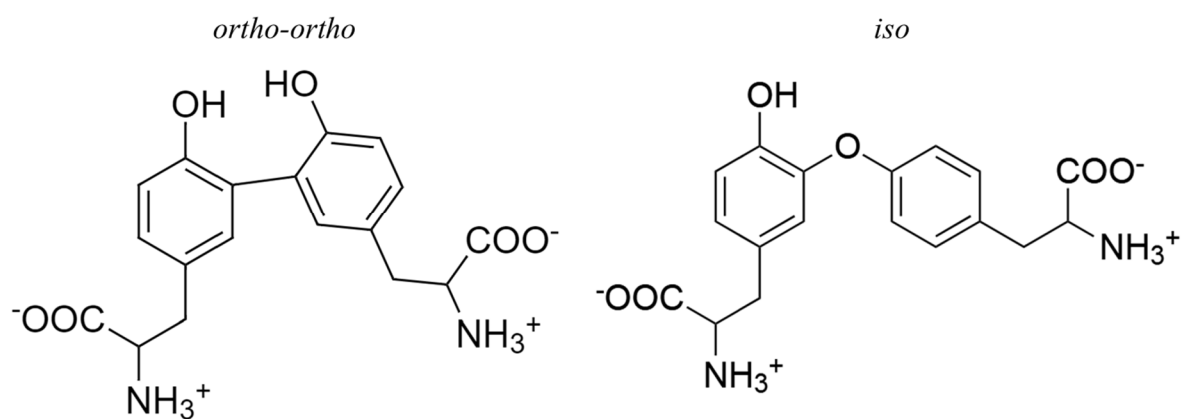


Figure 9: Full scan MS spectra of the four dimers of tyrosine extracted from Figure 8B.

# SCHEME 1



*Scheme 1: Schematic representation of already characterized di-tyrosine.*

## SCHEME 2

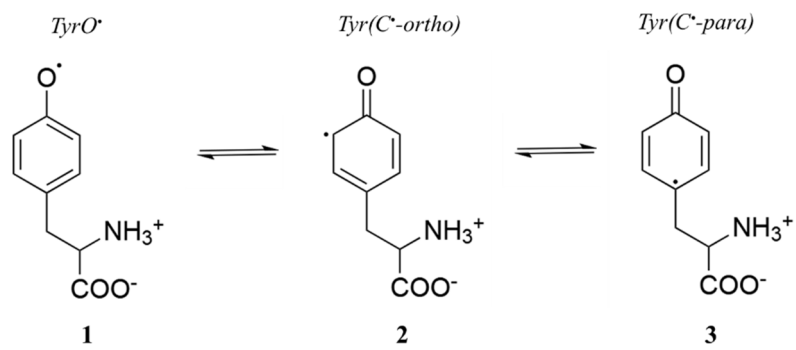


**TABLE 1**

Fragment (y)	<u>K</u> <u>T</u> <u>S</u> <u>L</u> <u>Y</u> - <u>K</u> <u>T</u> <u>S</u> <u>L</u> <u>Y</u>	<u>K</u> <u>T</u> <u>S</u> <u>L</u> <u>Y</u> - <u>T</u> <u>S</u> <u>L</u> <u>Y</u>	<u>K</u> <u>T</u> <u>S</u> <u>L</u> <u>Y</u> - <u>S</u> <u>L</u> <u>Y</u>	<u>K</u> <u>T</u> <u>S</u> <u>L</u> <u>Y</u> - <u>L</u> <u>Y</u>	<u>K</u> <u>T</u> <u>S</u> <u>L</u> <u>Y</u> - <u>Y</u>	<u>T</u> <u>S</u> <u>L</u> <u>Y</u> - <u>Y</u>	<u>S</u> <u>L</u> <u>Y</u> - <u>Y</u>	<u>L</u> <u>Y</u> - <u>Y</u>	<u>Y</u> - <u>Y</u>
<b>Protonated state charge (+)</b>	2	1	1	1	1	1	1	1	1
<b>Calculated <math>m/z</math></b>	610.332	1091.561	990.514	903.482	790.398	662.303	561.255	474.223	361.139
<b>Measured <math>m/z</math> (D<sub>1</sub>)</b>	610.367	1091.611	990.597	903.547	790.459	662.352	561.291	474.252	361.164
<b>Measured <math>m/z</math> (D<sub>2</sub>)</b>	610.367	1091.626	990.597	903.547	790.422	662.307	561.291	474.271	361.172
<b>Measured <math>m/z</math> (D<sub>3</sub>)</b>	610.377	1091.582	990.611	903.521	790.459	662.363	561.281	474.252	361.164
<b>Measured <math>m/z</math> (D<sub>4</sub>)</b>	610.377	1091.611	990.528	903.534	790.422	662.374	561.281	474.262	361.172
<b>Measured <math>m/z</math> (D<sub>5</sub>)</b>	610.377	1091.640	990.583	903.547	790.434	662.341	561.312	474.271	361.156

Table 1: MS-MS y fragments of di-KTSLY at  $m/z 610 \pm 1$  after irradiation at 40Gy with  $N_3^+$ . Calculated  $m/z$  ratio are compared to the measured ones.

## TABLE 2

<b>di-KTSLY</b>	<b>Digested</b>	<b>Digested</b>	<b>KTSLY</b>
	<b><math>\Delta 25</math> HO<sup>•</sup></b>	<b><math>\Delta 25</math> N<sub>3</sub><sup>•</sup></b>	<b>N<sub>3</sub><sup>•</sup></b>
D <sub>1</sub> <sup>2+</sup>	610.326	610.345	610.345
D <sub>2</sub> <sup>2+</sup>	610.337	610.326	610.334
D <sub>3</sub> <sup>2+</sup>	610.326	610.326	610.334
D <sub>4</sub> <sup>2+</sup>	610.337	610.326	610.334
D <sub>5</sub> <sup>2+</sup>	Not found	610.337	610.345

Table 2: Measured  $m/z$  values of di-KTSLY (calculated:  $m/z$  610.332) for the digested protein and synthetic KTSLY.